ACS central science

http://pubs.acs.org/journal/acscii

Research Article

Predicting the Plateau Modulus from Molecular Parameters of Conjugated Polymers

Abigail M. Fenton, Renxuan Xie, Melissa P. Aplan, Youngmin Lee, Michael G. Gill, Ryan Fair, Fabian Kempe, Michael Sommer, Chad R. Snyder, Enrique D. Gomez,* and Ralph H. Colby*

Cite This: *ACS Cent. Sci.* 2022, 8, 268–274

Read Online

ACCESS | Metrics & More | Article Recommendations | Supporting Information

ABSTRACT: The relationship between Kuhn length l_k, Kuhn monomer volume v_0, and plateau modulus G_N^0, initially proposed by Graessley and Edwards for flexible polymers, and extended by Everaers, has a large gap in experimental data between the flexible and stiff regimes. This gap prevents the prediction of mechanical properties from the chain structure for any polymer in this region. Given the chain architecture, including a semiflexible backbone and side chains, conjugated polymers are an ideal class of material to study this crossover region. Using small angle neutron scattering, oscillatory shear rheology, and the freely rotating chain model, we have shown that 12 polymers with aromatic backbones populate a large part of this gap. We also have shown that a few of these polymers exhibit nematic ordering, which lowers G_N^0. When fully isotropic, these polymers follow a relationship between l_k, v_0, and G_N^0, with a simple crossover proposed in terms of the number of Kuhn segments in an entanglement strand N_e.

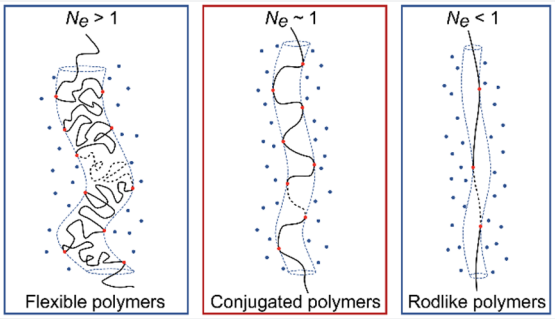

1. INTRODUCTION

Advances in technology and consumer electronics have progressed quickly from large stationary computers to portable and wearable technology, requiring flexible and stretchable biointegrated electronics. As human tissues and organs have low modulus, implanting electronic devices based on high modulus materials like silicon can have negative effects on the body, such as tissue scarring, device rejection due to inflammatory responses, and changes in cell division and growth in tissues around the device.[1−4] Conjugated polymers and gels range in mechanical modulus (Young's modulus, E) from 16 GPa to less than 100 kPa[4−6] and are much closer in stiffness to biological tissues than inorganic materials such as silicon (E of 130 GPa).[7] As such, devices based on conjugated polymers could be ideal for implantable bioelectronics.[8−10]

While semicrystalline conjugated polymers are often applied as the active layer of electronic devices, they are often too brittle and stiff for bio applications.[4] Instead, entangled amorphous conjugated polymers are an interesting class of material for use in soft and stretchable electronics; nevertheless, predicting the modulus for this class of materials remains a challenge.

Mechanical moduli of amorphous polymers above their glass transition temperature (T_g) are governed by entanglements, which are temporary physical cross-links in the polymer that create a plateau modulus (G_N^0) at time scales before the chains can unentangle and the modulus can further decrease. If G_N^0, Rouse time of an entanglement strand τ_e, and the molecular mass distribution of the material are known, one can use various polymer models to predict the time and temperature dependence of the mechanical modulus.[11] Relationships have been proposed for the prediction of mechanical properties from chain architecture[12] that, if verified for semiflexible conjugated polymers, could enable more efficient design of modulus-specific conjugated polymers for various applications, such as bioelectronics.

In 1981, Graessley and Edwards proposed a dimensionless relationship between the mechanical properties (G_N^0) and the chain dimensions of the polymer (Kuhn length, l_k, and Kuhn monomer volume, v_0)[13] that we recast as

$$\frac{G_N^0 v_0}{k_B T} = \left(\frac{l_k^3}{v_0}\right)^{\alpha} \quad (1)$$

where k_B is the Boltzmann constant. G_N^0 is inversely related to the entanglement molecular mass M_e as[14]

$$G_N^0 = \frac{\rho k_B T N_A}{M_e} \quad (2)$$

Received: November 12, 2021
Published: January 18, 2022

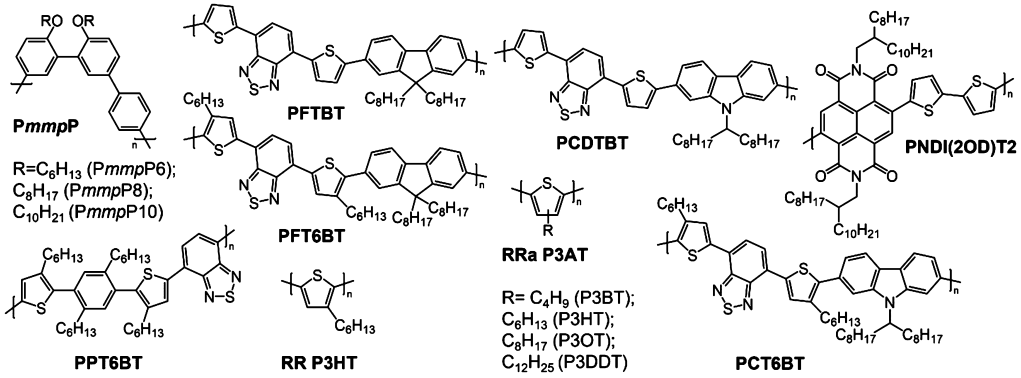

Figure 1. Chemical structures of conjugated polymers investigated in this study.

where ρ is the mass density and N_A is Avogadro's number. The Kuhn length, l_k, is the length scale that describes how the backbone correlations decay, and is a scale of local backbone rigidity. The Kuhn monomer volume, v_0, is how much space a Kuhn monomer occupies, and is described by[15−17]

$$v_0 = \frac{m_0}{\rho N_A}\frac{l_k}{l_0} \tag{3}$$

where m_0 and l_0 are the molar mass and length of the repeat unit, respectively.

Expressing this relationship in terms of v_0 instead of the more commonly used packing length (p), as seen previously,[17] leads to $G_N^0 v_0/k_B T = 1/N_e$, where N_e is the number of Kuhn monomers in an entanglement strand.[18] Thus, measurements of G_N^0 as a function of p (or v_0) lie on a universal curve when nondimensionalized as previously reported by Everaers; this single curve encompasses all polymers from the flexible regime to the stiff regime and is known as the Everaers plot.[12]

This relationship could be useful for designing new materials for modulus-specific applications, such as in organic bioelectronics. However, a large gap in experimental data between the flexible and stiff regimes exists, thereby limiting confidence in predictions within this crossover region. Conjugated polymers fall between flexible polymers and stiff polymers in the Everaers plot, and are thus a unique class of polymers that can be used to fill the gap. This verification would not only bring further insight into the inconsistencies between current scaling arguments as discussed by Hoy, Kroger, and Milner,[19,20] but also allow the use of the Everaers plot to develop modulus-specific polymers for various applications simply by knowing information about chain structure.

In this work, a systematic study of various entangled isotropic conjugated polymers with semiflexible chains were used to investigate the crossover regime between the flexible and stiff limits. A set of conjugated polymers designed to exhibit an isotropic phase over a wide range of temperatures and frequencies enables studies of entanglement when crystals or liquid crystallinity are not present (liquid crystalline phases such as the nematic phase, which is common in stiffer conjugated polymers, lowers the number of entanglements and therefore G_N^0).[21] Values for l_k from small angle neutron scattering (SANS) verify that the simple freely rotating chain model can accurately predict l_k for conjugated polymers with a wide range of backbone stiffnesses and flexible alkyl side chains. Using oscillatory shear rheology, we find that conjugated polymers appear to follow a universal relationship between chain properties (l_k and v_0) and mechanical properties (G_N^0), opening the door for future predictions of mechanical properties from the chemical structure.

2. RESULTS AND DISCUSSION

The chemical structures shown in Figure 1 were designed and synthesized to reduce crystallization through the addition of defects, by controlling regioregularity, adding steric hindrance, and breaking chain planarity through the addition of side chains, to span a wide range of backbone stiffnesses from flexible to semiflexible. PCT6BT, PFT6BT, and PPT6BT were designed to have increased steric hindrance and therefore reduced crystallinity due to an addition of hexyl side chains on the thiophene units. This steric hindrance can prevent close interactions between the aromatic backbones, disrupt $\pi-\pi$ stacking in the material, and thereby suppress crystallization. The regiorandom poly(3-alkylthiophenes) (RRa P3AT) have suppressed crystallinity due to a nonsymmetric repeat unit adding randomly, and these defects often prevent crystallization.[22−25] Keeping the backbone constant, such that l_k is invariant, but the side chains differ, as is the case in the RRa P3AT and the poly(*meta*,*meta*,*para*-phenylene) (P*mmp*P) series in Figure 1, allows tuning of v_0 independent of l_k. This offers the ability to fine-tune v_0 in hopes of populating a large area of the Everaers plot.

A series of experiments including differential scanning calorimetry (DSC) and oscillatory shear temperature ramp tests were conducted to investigate the phase behavior of these materials and ensure they are isotropic. DSC of the RRa P3AT's shows an absence of any melting or crystallization peaks in heating and cooling runs, respectively; this lack of first-order transitions in these materials suggests that they are amorphous. As rheology is more sensitive to microscopic changes in the material than DSC, it can more accurately investigate phase behavior.[26] In a common temperature ramp test, any crystallinity would appear as a flat solid-like plateau with a steep decrease in modulus upon melting. Rheology is also ideal for identifying the nematic to isotropic transition temperature (T_{NI}), as it is the only known cause for an increase in viscosity with temperature; this can be seen in SI 1 at 144 °C for PPT6BT.[21] Frequency sweeps and constructing master-curves using time−temperature superposition (tTs) can also reveal phase transitions in the material as areas where tTs fails. The absence of any crystallization or T_{NI} throughout the entire temperature range suggests isotropic behavior in PCT6BT and PFT6BT (see SI 2). In the case of PPT6BT (see SI 1), the T_{NI} occurred at 144 °C. Therefore, all subsequent measurements of this polymer were performed approximately 40 °C above this

https://doi.org/10.1021/acscentsci.1c01396
ACS Cent. Sci. 2022, 8, 268−274

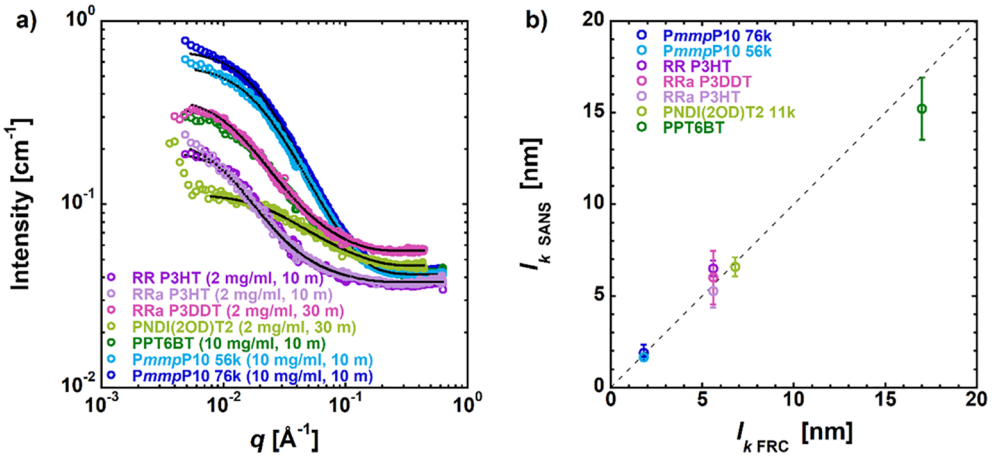

Figure 2. Kuhn lengths obtained from small angle neutron scattering (SANS) and the freely rotating chain model. (a) Typical SANS data for 7 conjugated or aromatic polymers dilute in d^5-chlorobenzene. Intensity is normalized to the scattering cross section and plotted vs scattering wavevector q. These data are fit to the flexible cylinder model using contour length and dispersity ($Đ$) obtained from polystyrene-standard calibrated gel permeation chromatography (GPC) and a fixed scattering length density. Fits are shown as black lines. (b) l_k's predicted by the FRC model ($l_{k\ FRC}$) are consistent with experimentally measured l_k's from SANS ($l_{k\ SANS}$) over a wide range of chain stiffnesses. Error bars are the best representation of 1 standard deviation in the experimental uncertainty.

Table 1. Chain Dimensions, Polymer Properties, and Plateau Moduli for Various Conjugated Polymers

polymer	l_k [nm] FRC	l_k [nm] SANS	T [°C]	l_0 [nm][a]	m_0 [kg/mol]	v_0 [nm^3]	l_k^3/v_0	G_N^0 [MPa][g]	M_e [kg/mol]	N_e	τ_e [μs]	ρ [g/cm^3][h]	M_w [kg/mol]	$Đ$
P*mmp*P10	1.8	1.9 ± 0.5	200	1.2	0.54	1.45[b]	4.7	0.29	13.0	15	5.0	0.96	76	1.8
P*mmp*P8	1.8		200	1.2	0.48	1.30[b]	5.3	0.48	7.9	11	10	0.96	73	2.1
P*mmp*P6	1.8		240	1.2	0.43	1.15[b]	6.0	0.85	4.8	7.2	2.8	0.96	109	2.1
RRa P3DDT	5.6	6.0 ± 1.5	200	0.40	0.25	5.99[c]	29	0.46	8.4	2.4	0.3	0.98	79	1.8
RRa P3OT	5.6		240	0.40	0.19	5.24[c]	34	0.67	5.6	2.0	0.16	0.87	62	2.8
RRa P3HT	5.6	5.3 ± 0.9	240	0.40	0.17	3.55[c]	49	0.81	5.8	2.5	0.7	1.1	110	3.1
RRa P3BT	5.6		240	0.40	0.14	3.27[c]	52	1.01	4.1	2.1	0.7	0.98	72	2.5
PFT6BT	11		240	2.1	0.85	7.99[c]	167	0.75	5.3	1.2	60	0.94	66	2.3
PFTBT	11		300	2.1	0.67	4.47[c]	298	0.43[e]	15	4.0	100	1.35	135	4.2
PCT6BT	12		140	2.1	0.87	8.42[c]	195	0.55	6.1	1.2	12000	0.98	36	1.8
PCDTBT	12		300	2.1	0.70	5.55[c]	296	0.21[e]	27	7.0	430	1.2	200	3.7
PPT6BT	17	15 ± 1.7	200	1.7	0.71	11.6[d]	304	0.46[f]	8.0	1.2	500	0.94	49	1.6

[a] l_0 values obtained using Avogadro.[32] [b] v_0 evaluated using l_k from SANS for P*mmp*P10 obtained at 25 °C. [c] v_0 evaluated using l_k from the FRC model. [d] v_0 evaluated using l_k from SANS obtained at 25 °C. [e] G_N^0 for PFTBT and PCDTBT are taken from fitting the master-curves just above their T_{NI}'s, so some nematic effects are expected. [f] Isotropic G_N^0 for PPT6BT was obtained by shifting to a reference temperature ~60 °C above the T_{NI}. [g] G_N^0 for all polymers from fits to BoB. [h] ρ for each polymer was obtained at the reference temperatures listed in the table.

temperature to ensure the material was fully isotropic. Thus, large temperature ranges where the polymers in Figure 1 were above the T_g and also isotropic were identified.[27] For PFTBT and PCDTBT, T_{NI}'s occur at 290 and 273 °C, respectively. As it is difficult to measure 40 °C above these temperatures without the risk of degradation, these polymers still contain some nematic local alignment at the measurement temperature of 300 °C.[21]

To verify that these polymers lie in the semiflexible gap of the Everaers plot, their Kuhn lengths were determined. The freely rotating chain model (FRC)[18] has been used to predict l_k from the chemical structure of conjugated molecules.[28] The FRC model requires information about the structure, such as bond lengths and bond angles, but assumes the dihedral angles rotate freely, with sufficiently long chain lengths so that l_k is independent of chain length. While the FRC model has been used successfully to predict the l_k of a few semiflexible polymers, it has not been verified for polymers with l_k's larger than 11 nm.[28] We verify the FRC using SANS from dilute solutions of P*mmp*P10 (56 kg/mol and 76 kg/mol), PPT6BT, PNDI(2OD)T2, RR P3HT, RRa P3HT, and RRa P3DDT. Data were acquired using the 10 and 30 m SANS beamlines at the Center for Neutron Research (NCNR) at the National Institute of Standards and Technology (NIST) and were fit to a flexible cylinder model[29] in SasView[30] using Levenberg–Marquardt fitting with 10^5 steps per fit, as shown in Figure 2a. As shown in Figure 2b, the FRC model accurately predicts l_k for the polymers tested in the range $1.8 \leq l_k \leq 15$ nm (see Table 1).

Having obtained values for l_k, v_0 can be obtained using eq 3 in combination with the mass density. The density was measured by melt-casting a bubble-free puck of known mass and measuring its height and diameter in a rheometer at various temperatures (Table 1). The Kuhn monomer volumes span a wide range of the flexible to semiflexible regime, allowing the conjugated polymers chosen for this study to

https://doi.org/10.1021/acscentsci.1c01396
ACS Cent. Sci. 2022, 8, 268−274

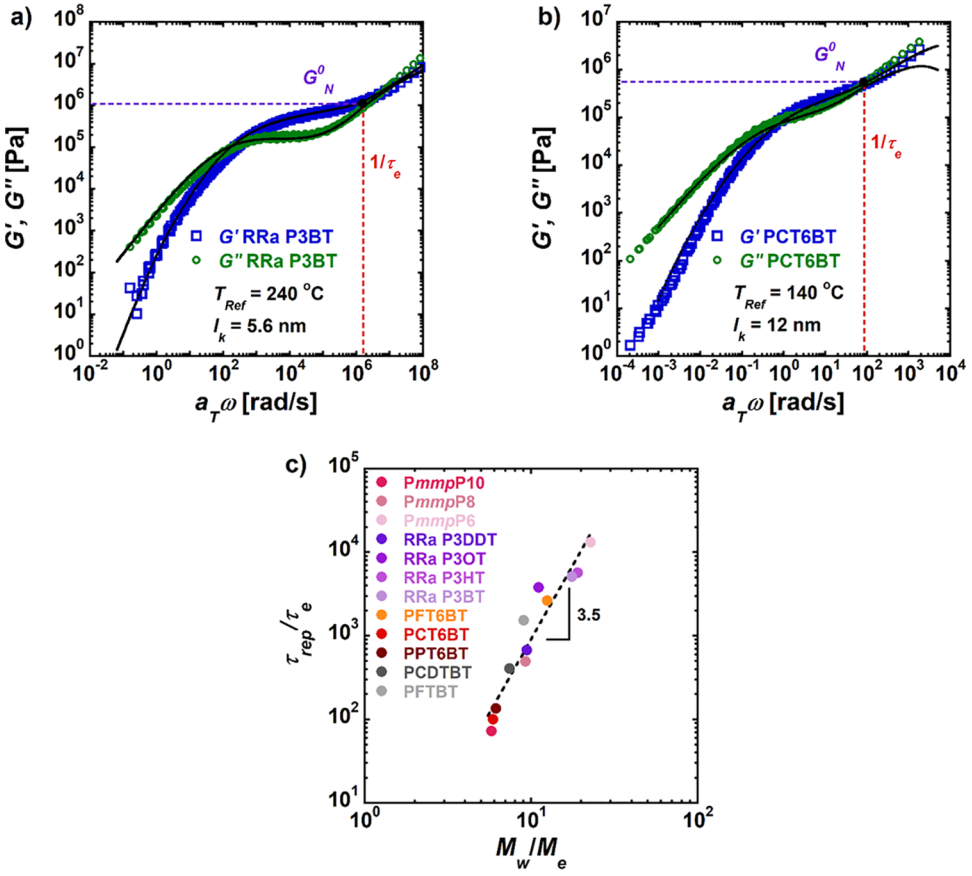

Figure 3. Master-curves of (a) RRa P3BT and (b) PCT6BT. Master-curves were generated using tTs and were horizontally shifted to reference temperatures of 240 and 140 °C, respectively, using shift factors a_T as shown in SI 6−9. The open symbols are experimental data, and the solid black curves are the fits to G' and G'', generated from the BoB tube model, inputting the molecular mass distribution from GPC and assuming all chains are linear. The master-curves for the other 10 polymers tested can be seen in SI 3−5. (c) Ratio of the reptation time, τ_{rep}, and Rouse time of an entanglement strand, τ_e, as a function of the number of entanglements along the chain for all 12 conjugated polymers.

populate the gap of the Everaers plot. To know whether these polymers follow the relationship between l_k, ν_0, and G_N^0, however, requires a measurement of the plateau modulus.

Oscillatory frequency sweeps were taken over a wide range of temperatures and shifted using tTs to generate master-curves for each polymer in the isotropic liquid state (master-curves and shift factors can be seen in SI 3−9). G_N^0 can be approximated by taking the modulus value at the high frequency crossing of the storage modulus (G') and loss modulus (G'') at the Rouse time of an entanglement strand, τ_e. As these polymers have high dispersity, fitting the master-curves to a tube model is needed for quantification. Herein we use the Branch-on-Branch (BoB) model developed by Das et al.[11] with molecular mass distribution as an input (weight-average molecular mass, M_w, and dispersity, $Đ$, can be seen in Table 1), assuming that all chains are linear and that the tube diameter is larger than l_k (meaning that the number of Kuhn monomers in an entanglement strand $N_e > 1$). These assumptions are met for the polymers presented in this study, allowing for fitting master-curves to BoB to obtain the entanglement molecular mass and G_N^0. Two master-curves can be seen in Figure 3a and b (others are in SI 3−5). As expected, the BoB fits are best at lower l_k; as the polymer gets stiffer BoB cannot be expected to accurately report G_N^0, because the polymer entanglements are starting to be governed more by bending and strong reptation than Rouse motion (see SI 10).[31] Nevertheless, these polymers approximately follow the experimental scaling relationship of 3.4 between τ_e, the reptation time, τ_{rep}, and the number of entanglements per chain, as seen in Figure 3c.[18] This shows that the usual relation between the rubbery plateau width and the number of entanglements per chain still applies for the 12 conjugated polymers of this study, and their master-curves can therefore be fitted using the BoB model. Approximations of G_N^0 by taking the crossover modulus at τ_e (the high frequency end of the plateau) are also in reasonable agreement with the predictions of G_N^0 from BoB, as expected for polymers whose entanglements are governed by Rouse motion. Values of G_N^0, M_e, and τ_e can be seen in Table 1.

Using eq 1, we show that aromatic and conjugated polymers populate a wide range between the flexible and stiff regimes. In addition, we can explore whether the previously reported Kremer−Grest bead−spring scaling models proposed by Uchida et al.[12] accurately represent the crossover regime between stiff and flexible chains. Aromatic P*mmp*P polymers follow Lin-Noolandi scaling with a power law exponent (see eq 1) $\alpha = 2$, which suggests that these polymers are flexible.[33,34] The P3AT, PFT6BT, and PCT6BT and PPT6BT polymers follow closer to the Morse scaling with a power law exponent $\alpha = 2/5$, indicating that these conjugated polymers are semiflexible and are a unique class of materials.[35] Based on these data, we propose a simple crossover equation between the two regimes (eq 4).

https://doi.org/10.1021/acscentsci.1c01396
ACS Cent. Sci. 2022, 8, 268−274

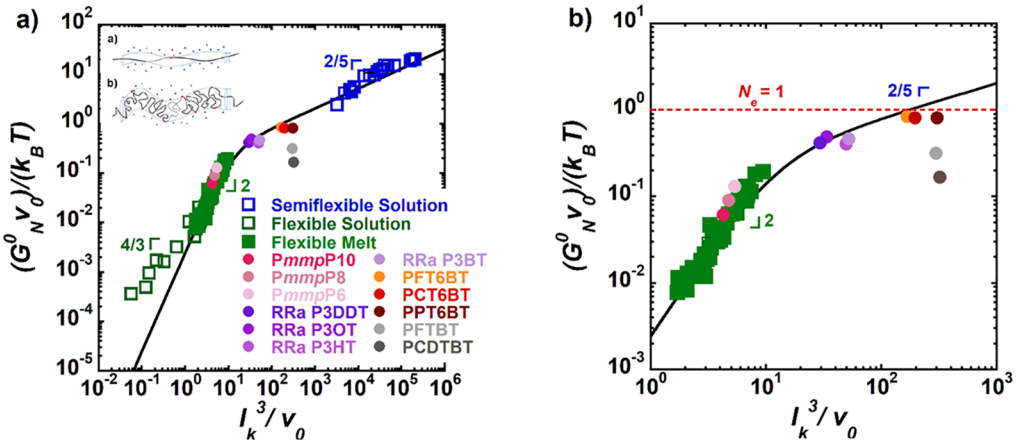

Figure 4. Conjugated polymer melts (circles) follow Everaers' scaling predictions with dimensionless plateau modulus G_N^0 vs dimensionless Kuhn monomer volume v_0. (a) Flexible melt data (solid green squares) were obtained from refs 15 and 37, the flexible solution data (open green squares) from refs 38 and 39, and the semiflexible solution data (open blue squares) were obtained from refs 40 and 41. The solid black line is the proposed crossover given by eq 4. The more flexible P*mmp*P polymers fit best with the flexible melt scaling argument $(l_k^3/v_0)^2$ while P3AT, PFT6BT, and PCT6BT and PPT6BT fit best with the semiflexible scaling argument of $(l_k^3/v_0)^{2/5}$. The PFTBT and PCDTBT polymers lie well below the prediction; this is hypothesized to be due to lingering nematic domains slightly above their T_{NI}. The tube model for a semiflexible and flexible polymer can be seen in insets (a) and (b), respectively. (b) Expanded view of the crossover region. The dashed red line indicates $N_e = 1$.

$$N_e = \frac{k_B T}{G_N^0 v_0} = 400\left(\frac{l_k^3}{v_0}\right)^{-2} + 7.77\left(\frac{l_k^3}{v_0}\right)^{-2/5} \quad (4)$$

Equation 4 suggests that the crossover between the flexible and stiff regimes is controlled by l_k and v_0. The values for the crossover can be obtained by equating the two terms in eq 4, such that the crossover occurs at $l_k^3/v_0 = 11.7$ with $N_e = 5.8$, which is significantly larger than unity. This crossover equation fits the semiflexible regime well (see Figure 4) when compared to the bead−spring models presented by Uchida et al.[12] that do not accurately fit semiflexible melts.[19] Hoy et al. recently have refined their original bead−spring model using molecular dynamics and topological analyses.[36] This refined model, which outperforms previously proposed expressions, fits quite well with the proposed crossover equation presented in this paper.[36]

PFTBT and PCDTBT lie well below the prediction, which suggests that lingering local nematic alignment may persist in these materials slightly above their T_{NI}. As the degradation temperature for many conjugated polymers begins just above 300 °C, and the T_{NI} for both PFTBT and PCDTBT are above 270 °C, it is likely that both polymers are not fully isotropic and therefore have reduced entanglements as previously shown.[21] In the case of PPT6BT, which also has a nematic phase but does follow Everaers' prediction, the T_{NI} is far below the degradation temperature. This allows us to measure the polymer well above its T_{NI}, deep into the isotropic phase.

3. CONCLUSIONS

We have verified the use of the FRC model and experimentally populated the previously empty crossover between flexible and stiff polymers, thereby validating scaling theories in this region and demonstrating that the Everaers relationship can be used to predict G_N^0 of conjugated polymers from their structure. Conjugated polymers are semiflexible, enabling our study of the crossover between the flexible and stiff regimes. These results re-emphasize the importance of identifying how nematic phases can affect not only the charge transport properties of conjugated polymers but also entanglements, and therefore mechanical properties as well. Figure 4 provides a universal curve that allows predictions of mechanical moduli for chains of various backbone stiffnesses from l_k. Furthermore, in conjunction with linear viscoelastic descriptions (such as BoB), Figure 4 can allow the generation of rheological spectra that would provide insight to other mechanical aspects of any polymer, such as relaxation and terminal behavior. For melts of strictly linear chains, G_N^0, M_e, and τ_e are the only material parameters needed once molecular weight distribution is measured. Ultimately, this work helps enable the prediction of mechanical properties of isotropic conjugated polymers to support the design of stretchable and biocompatible electronics.

■ ASSOCIATED CONTENT

Supporting Information

The Supporting Information is available free of charge at https://pubs.acs.org/doi/10.1021/acscentsci.1c01396.

Figures, detailed experimental methods, and analysis including information on polymer synthesis, phase behavior analysis using temperature ramps and frequency sweeps, SANS data, as well as master-curves and BoB fits for all polymers studied (PDF)

■ AUTHOR INFORMATION

Corresponding Authors

Enrique D. Gomez − *Department of Chemical Engineering, Department of Materials Science and Engineering, and Materials Research Institute, The Pennsylvania State University, University Park, Pennsylvania 16802, United States;* orcid.org/0000-0001-8942-4480; Email: edg12@psu.edu

Ralph H. Colby − *Department of Materials Science and Engineering and Materials Research Institute, The Pennsylvania State University, University Park, Pennsylvania 16802, United States;* orcid.org/0000-0002-5492-6189; Email: rhc5@psu.edu

https://doi.org/10.1021/acscentsci.1c01396
ACS Cent. Sci. 2022, 8, 268−274

Authors

Abigail M. Fenton − *Department of Chemical Engineering, The Pennsylvania State University, University Park, Pennsylvania 16802, United States*

Renxuan Xie − *Department of Chemical Engineering, The Pennsylvania State University, University Park, Pennsylvania 16802, United States*

Melissa P. Aplan − *Department of Chemical Engineering, The Pennsylvania State University, University Park, Pennsylvania 16802, United States*

Youngmin Lee − *Department of Chemical Engineering, The New Mexico Institute of Mining and Technology, Socorro, New Mexico 87801, United States;* orcid.org/0000-0002-7402-8829

Michael G. Gill − *Department of Chemical Engineering, The Pennsylvania State University, University Park, Pennsylvania 16802, United States*

Ryan Fair − *Department of Materials Science and Engineering, The Pennsylvania State University, University Park, Pennsylvania 16802, United States*

Fabian Kempe − *Institute for Chemistry, Chemnitz University of Technology, 09111 Chemnitz, Germany*

Michael Sommer − *Institute for Chemistry, Chemnitz University of Technology, 09111 Chemnitz, Germany;* orcid.org/0000-0002-2377-5998

Chad R. Snyder − *Materials Science and Engineering Division, National Institute of Standards and Technology, Gaithersburg, Maryland 20899, United States*

Complete contact information is available at: https://pubs.acs.org/10.1021/acscentsci.1c01396

Notes

Certain commercial equipment, instruments, or materials are identified in this paper in order to specify the experimental procedure accurately. Such identification is not intended to imply recommendation or endorsement by the National Institute of Standards and Technology, nor is it intended to imply that the materials or equipment identified are necessarily the best available for the purpose.

The authors declare no competing financial interest.

■ ACKNOWLEDGMENTS

The authors thank Scott T. Milner and Robert S. Hoy for helpful comments. Funding support from the National Science Foundation under award numbers DMR-1629006 and DMR-1921854 is gratefully acknowledged. The authors thank R. Matsidik for synthesizing the PNDI(2OD)T2 sample. We acknowledge the support of the National Institute of Standards and Technology, U.S. Department of Commerce, for providing the neutron research facilities used in this work. Use of the NG-B 10 m SANS instrument was supported by the NIST nSoft Consortium.

■ REFERENCES

(1) Levental, I.; Georges, P. C.; Janmey, P. A. Soft biological materials and their impact on cell function. *Soft Matter* **2007**, *3* (3), 299−306.

(2) Sohal, H. S.; Clowry, G. J.; Jackson, A.; O'Neill, A.; Baker, S. N. Mechanical Flexibility Reduces the Foreign Body Response to Long-Term Implanted Microelectrodes in Rabbit Cortex. *PLoS One* **2016**, *11* (10), e0165606.

(3) Yuk, H.; Lu, B.; Zhao, X. Hydrogel bioelectronics. *Chem. Soc. Rev.* **2019**, *48* (6), 1642−1667.

(4) Liu, Y.; Liu, J.; Chen, S.; Lei, T.; Kim, Y.; Niu, S.; Wang, H.; Wang, X.; Foudeh, A. M.; Tok, J. B.; Bao, Z. Soft and elastic hydrogel-based microelectronics for localized low-voltage neuromodulation. *Nat. Biomed Eng.* **2019**, *3* (1), 58−68.

(5) Savagatrup, S.; Makaram, A. S.; Burke, D. J.; Lipomi, D. J. Mechanical Properties of Conjugated Polymers and Polymer-Fullerene Composites as a Function of Molecular Structure. *Adv. Funct. Mater.* **2014**, *24* (8), 1169−1181.

(6) Lu, B.; Yuk, H.; Lin, S.; Jian, N.; Qu, K.; Xu, J.; Zhao, X., Pure PEDOT:PSS hydrogels. *Nat. Commun.* **2019**, *10* (1). DOI: 10.1038/s41467-019-09003-5

(7) Someya, T.; Bao, Z.; Malliaras, G. G. The rise of plastic bioelectronics. *Nature* **2016**, *540* (7633), 379−385.

(8) Zeglio, E.; Rutz, A. L.; Winkler, T. E.; Malliaras, G. G.; Herland, A. Conjugated Polymers for Assessing and Controlling Biological Functions. *Adv. Mater.* **2019**, *31* (22), 1806712.

(9) Rivnay, J.; Owens, R. M.; Malliaras, G. G. The Rise of Organic Bioelectronics. *Chem. Mater.* **2014**, *26* (1), 679−685.

(10) Liao, C.; Zhang, M.; Yao, M. Y.; Hua, T.; Li, L.; Yan, F. Flexible Organic Electronics in Biology: Materials and Devices. *Adv. Mater.* **2015**, *27* (46), 7493−7527.

(11) Das, C.; Inkson, N. J.; Read, D. J.; Kelmanson, M. A.; McLeish, T. C. B. Computational linear rheology of general branch-on-branch polymers. *J. Rheol.* **2006**, *50*, 207−207.

(12) Uchida, N.; Grest, G. S.; Everaers, R., Viscoelasticity and primitive path analysis of entangled polymer liquids: From F-actin to polyethylene. *J. Chem. Phys.* **2008**, *128* (4).044902

(13) Graessley, W. W.; Edwards, S. F. Entanglement interactions in polymers and the chain contour concentration. *Polymer* **1981**, *22* (10), 1329−1334.

(14) Doi, M.; Edwards, S. F. *The Theory of Polymer Dynamics*. Clarendon Press: 1986; p 391−391.

(15) Fetters, L. J.; Lohse, D. J.; Richter, D.; Witten, T. A.; Zirkel, A. Connection between Polymer Molecular-Weight, Density, Chain Dimensions, and Melt Viscoelastic Properties. *Macromolecules* **1994**, *27* (17), 4639−4647.

(16) Fetters, L. J.; Lohse, D. J.; Graessley, W. W. Chain dimensions and entanglement spacings in dense macromolecular systems. *J. Polym. Sci., Part B: Polym. Phys.* **1999**, *37* (10), 1023−1033.

(17) Everaers, R.; Sukumaran, S. K.; Grest, G. S.; Svaneborg, C.; Sivasubramanian, A.; Kremer, K. Rheology and Microscopic Topology of Entangled Polymeric Liquids. *Science* **2004**, *303* (5659), 823−826.

(18) Rubinstein, M.; Colby, R. H. *Polymer Physics.*; Oxford University Press: 2003; p 440−440.

(19) Hoy, R. S.; Kroger, M. Unified Analytic Expressions for the Entanglement Length, Tube Diameter, and Plateau Modulus of Polymer Melts. *Phys. Rev. Lett.* **2020**, *124* (14), 147801.

(20) Milner, S. T. Unified Entanglement Scaling for Flexible, Semiflexible, and Stiff Polymer Melts and Solutions. *Macromolecules* **2020**, *53* (4), 1314−1325.

(21) Xie, R.; Aplan, M. P.; Caggiano, N. J.; Weisen, A. R.; Su, T.; Müller, C.; Segad, M.; Colby, R. H.; Gomez, E. D. Local Chain Alignment via Nematic Ordering Reduces Chain Entanglement in Conjugated Polymers. *Macromolecules* **2018**, *51* (24), 10271−10284.

(22) Pankaj, S.; Beiner, M. Long-term behavior and side chain crystallization of poly(3-alkyl thiophenes). *Soft Matter* **2010**, *6* (15), 3506−3516.

(23) Zhan, P.; Zhang, W.; Jacobs, I. E.; Nisson, D. M.; Xie, R.; Weissen, A. R.; Colby, R. H.; Moulé, A. J.; Milner, S. T.; Maranas, J. K.; Gomez, E. D. Side chain length affects backbone dynamics in poly(3-alkylthiophene)s. *J. Polym. Sci., Part B: Polym. Phys.* **2018**, *56* (17), 1193−1202.

(24) Xie, R.; Colby, R. H.; Gomez, E. D., Connecting the Mechanical and Conductive Properties of Conjugated Polymers. *Advanced Electronic Materials* **2018**, *4* (10).1700356

(25) Snyder, C. R.; Henry, J. S.; DeLongchamp, D. M. Effect of Regioregularity on the Semicrystalline Structure of Poly(3-hexylthiophene). *Macromolecules* **2011**, *44* (18), 7088−7091.

(26) Xie, R.; Lee, Y.; Aplan, M. P.; Caggiano, N. J.; Müller, C.; Colby, R. H.; Gomez, E. D. Glass Transition Temperature of Conjugated Polymers by Oscillatory Shear Rheometry. *Macromolecules* **2017**, *50* (13), 5146−5154.
(27) Xie, R.; Weisen, A. R.; Lee, Y.; Aplan, M. A.; Fenton, A. M.; Masucci, A. E.; Kempe, F.; Sommer, M.; Pester, C. W.; Colby, R. H.; Gomez, E. D. Glass transition temperature from the chemical structure of conjugated polymers. *Nat. Commun.* **2020**, *11* (1), 4−11.
(28) Zhang, W.; Gomez, E. D.; Milner, S. T. Predicting Chain Dimensions of Semiflexible Polymers from Dihedral Potentials. *Macromolecules* **2014**, *47* (18), 6453−6461.
(29) Pedersen, J. S.; Schurtenberger, P. Scattering Functions of Semiflexible Polymers with and without Excluded Volume Effects. *Macromolecules* **1996**, *29* (23), 7602−7612.
(30) *SasView*, 4.2.2.
(31) Faller, R.; Müller-Plathe, F. Chain Stiffness Intensifies the Reptation Characteristics of Polymer Dynamics in the Melt. *ChemPhysChem* **2001**, *2* (3), 180−184.
(32) *Avogadro: an open-source molecular builder and visualization tool.*, Version 1.2.1.
(33) Lin, Y. H. Number of entanglement strands per cubed tube diameter, a fundamental aspect of topological universality in polymer viscoelasticity. *Macromolecules* **1987**, *20* (12), 3080−3083.
(34) Kavassalis, T. A.; Noolandi, J. New View of Entanglements in Dense Polymer Systems. *Phys. Rev. Lett.* **1987**, *59* (23), 2674−2677.
(35) Morse, D. D., Tube diameter in tightly entangled solutions of semiflexible polymers. *Phys. Rev. E* **2001**, *63* (3). DOI: 10.1103/PhysRevE.63.031502
(36) Dietz, J. D.; Kroger, M.; Hoy, R. S., Validation and refinement of unified analytic model for flexible and semiflexible polymer melt entanglement. *Submitted*.
(37) Sukumaran, S. K.; Grest, G. S.; Kremer, K.; Everaers, R. Identifying the primitive path mesh in entangled polymer liquids. *J. Polym. Sci., Part B: Polym. Phys.* **2005**, *43* (8), 917−933.
(38) Inoue, T.; Yamashita, Y.; Osaki, K. Viscoelasticity of an Entangled Polymer Solution with Special Attention on a Characteristic Time for Nonlinear Behavior. *Macromolecules* **2002**, *35* (5), 1770−1775.
(39) Colby, R. H.; Fetters, L. J.; Funk, W. G.; Graessley, W. W. Effects of concentration and thermodynamic interaction on the viscoelastic properties of polymer solutions. *Macromolecules* **1991**, *24* (13), 3873−3882.
(40) Hinner, B.; Tempel, M.; Sackmann, E.; Kroy, K.; Frey, E. Entanglement, Elasticity, and Viscous Relaxation of Actin Solutions. *Phys. Rev. Lett.* **1998**, *81* (12), 2614−2617.
(41) Schmidt, F. G.; Hinner, B.; Sackmann, E.; Tang, J. X. Viscoelastic properties of semiflexible filamentous bacteriophage fd. *Phys. Rev. E* **2000**, *62* (4), 5509−5517.

https://doi.org/10.1021/acscentsci.1c01396
ACS Cent. Sci. 2022, 8, 268−274